Analysis of Solar Effects Upon Observed Doppler Noise During the Helios 1 Second Solar Conjunction

A. L. Berman
Network Operations Office

This report analyzes observed doppler noise during the Helios 1 second solar conjunction with the previously presented $NOISE_p$ solar noise model. It is concluded that the $NOISE_p$ model continues to adequately predict "average" solar corruption of observed doppler noise, and that deviations from the $NOISE_p$ model continue to appear to correlate in some fashion with fluctuations in observed solar activity.

I. Introduction

During August 1975, the Helios 1 spacecraft underwent its second solar conjunction. Previous to this event, this author and S. T. Rockwell, using doppler noise data gathered during the first Helios 1 solar conjunction (May 1975) and the 1975 Pioneer 10 (April) and Pioneer 11 (March) solar conjunctions, derived a geometrical parameter (ISI) which could be used to model solar corruption of doppler noise (Ref. 1). The model developed ($NOISE_p$) is as follows:

α = Sun-Earth-probe angle (SEP), deg

β = Earth-Sun-probe angle (ESP), deg

$$ISI = \frac{\beta}{\sin \alpha}$$

and:

$$NOISE_p\,(\text{Hz}) = \begin{cases} 0.003 & ; \quad ISI \leq 223 \\ K_1\,(ISI)^{1+K_2}; & ISI > 223 \end{cases}$$

where

$$K_1 = 2.8 \times 10^{-6}$$

$$K_2 = 2.9 \times 10^{-1}$$

Although the $NOISE_p$ model fit the early 1975 Helios 1, Pioneer 10 and Pioneer 11 solar conjunction doppler noise data in a reasonable fashion, it might be considered with some suspicion since the quantities K_1 and K_2 were empirically determined from the data. Therefore, the second 1975 Helios 1 solar conjunction represented the first

opportunity to test the $NOISE_p$ model against a solar conjunction data base entirely disassociated from the original derivation of the model. Obviously, a successful prediction of the Helios 1 second solar conjunction by the $NOISE_p$ model would auger well for the basic validity of the model.

Additionally, this author and S. T. Rockwell (Ref. 2) concluded that deviations from the $NOISE_p$ model could be explained by short-term fluctuations in solar activity; certainly one would be interested in again attempting to correlate solar activity with deviations from the $NOISE_p$ model. The main thrust of this report will hence address the following questions.

(1) How well does the $NOISE_p$ model fit the Helios 1 second solar conjunction doppler noise data?

(2) During the Helios 1 second solar conjunction, can deviations from the $NOISE_p$ model be correlated with observed fluctuations in solar activity?

II. Helios 1 Second Solar Conjunction Doppler Noise Data Base

The Helios 1 second solar conjunction phase climaxed with solar occultation on August 30 and 31, 1975. To substantially bracket this event, doppler noise data were accumulated from July 29, 1975 (DOY 210) to October 2, 1975 (DOY 275), inclusive. The data consist of an "average doppler noise" value for each pass (tracked) during the above period. Obviously, then, each "average doppler noise" value is completely specified by two parameters:

(1) Deep Space Station (DSS).

(2) Pass (actual starting DOY of pass).

The method used to select a "pass average" was changed slightly from Ref. 1 (p. 232) in an attempt to insure greater objectivity. The method used here was to record a doppler data running standard deviation each half hour throughout a track, from the Network Operations Control Center (NOCC) pseudoresidual program output. The six lowest values from each track were then averaged to produce the "pass average." Data were, of course, restricted to good, two-way, 60-second-sample-rate doppler data.

The accumulated data comprise Table 1. Presented in this table are the following parameters:

(1) Station (DSS).

(2) DOY (day of year of start of pass).

(3) Average noise (Hz).

(4) α (degrees).

(5) β (degrees).

(6) ISI (unitless).

III. Comparison of the $NOISE_p$ Model With Observed Doppler Noise During the Helios 1 Second Solar Conjunction

Figure 1 presents the $NOISE_p$ model and the observed doppler noise ($NOISE_A$) as a function of day of year (DOY), while Fig. 2 presents the same quantities as a function of SEP. Finally, Fig. 3 presents the observed doppler noise vs integrated solar intensity (ISI). Since the observed data show a pronounced positive bias when compared to the $NOISE_p$ model (which will be considered in Section IV to follow), the quantity

$$1.5 \times NOISE_p$$

has additionally been included in Figs. 1, 2, and 3. Examination of Figs. 1, 2, and 3 would certainly lead one to conclude in a qualitative sense that the $NOISE_p$ model is a good representation for the very disparate doppler noise data base accumulated during the Helios 1 second solar conjunction. However, it would be useful to attempt to make a more quantitative statement in regard to the efficacy of the $NOISE_p$ model as applied to the aforementioned data base. To this end, residuals were formed as follows:

$$\text{Residual} = 10 \log_{10}\left(\frac{NOISE_A}{1.5 \times NOISE_p}\right)$$

Residuals computed in the above manner for the Helios 1 second solar conjunction yielded the following standard deviation:

$$1\sigma = 2.15$$

which is to say that approximately 67% of the observed doppler noise values was constrainted to:

$$0.61\,[1.5 \times NOISE_p] < \text{Observed Noise} < 1.64\,[1.5 \times NOISE_p]$$

In consideration of the above, it is important to remember that the data base spans more than three orders of magnitude (0.0018 Hz to 5.000 Hz), or in logrithmic form:

$$10 \log_{10} \left\{ \frac{5.000}{0.0018} \right\} = 34.4$$

This author considers the $NOISE_p$ model performance creditable when the 1σ value of 2.15 is compared to a total range of 34.4, particularly in light of the nonexistence of any solar noise models prior to $NOISE_p$.

An allied subject invites comment at this time. B. Madsen (Ref. 3, p. 28) comments on the possibility of discrete solar events which might cause doppler noise at a SEP = 15 deg to increase to values expected at a SEP = 1 or 2 deg. At least as far as "pass average doppler noise" is concerned, this effect is not borne out by the data accumulated so far in Refs. 1 and 2 and this report. For instance, the residual of $NOISE_p$ at SEP = 1 deg compared to $NOISE_p$ at SEP = 15 deg is:

$$10 \log_{10} \left\{ \frac{NOISE_p(1°)}{NOISE_p(15°)} \right\} = 15.1$$

No residuals of this size have been observed for data in the region:

$$\text{SEP} \gtrsim 15 \text{ deg}$$

Finally, to further illustrate this point, Fig. 4 indicates the equivalent SEP angles for 1σ deviations from the $NOISE_p$ model, where

$$1\sigma = 2.15$$

IV. Correlation of $NOISE_p$ Residuals With Fluctuations in Solar Activity

In Ref. 2, it was concluded that deviations from the $NOISE_p$ model are primarily due to fluctuations in solar activity as seen along the signal path, these fluctuations being a result of

(1) Radial asymmetry of solar activity combined with solar rotation.

(2) Variation with time of solar activity for any region of the solar surface.

A particularly dramatic example of Item (1) can be seen in Fig. 5. Prior to DOY 084 (Pioneer 11 solar conjunction) both Pioneer 10 and Pioneer 11 signal paths were to the left (or east, as viewed from Earth) of the Sun; between DOY 084 and DOY 094 (Pioneer 10 solar conjunction), the Pioneer 10 signal path was to the left of the Sun and the Pioneer 11 signal path to the right (west) of the Sun; finally, after DOY 094, both Pioneer signal paths were again on the same side of the Sun (the west). Figure 5 shows the correlation to be very strong when both spacecraft signal paths are on the same side of the Sun, and little or no correlation when the spacecraft signal paths are on opposite sides of the Sun. Additionally, Fig. 5 indicates observed sunspot activity (Zurich, R_Z) which has been retarded 10 days for signal paths east of the Sun and advanced 10 days for signal paths west of the Sun. As was mentioned in Ref. 2, all indices of solar activity move somewhat in unison; Ref. 2 used Ottawa measured solar flux to indicate possible correlation with solar activity; this report will use R_Z for the same purpose.

Figure 6 shows the Helios 1 second solar conjunction $NOISE_p$ residuals plotted with R_Z (advanced 16 days for west signal paths and retarded 16 days for east signal paths) vs day of year. As in Ref. 2, strong similarities are seen between the residuals and solar (sunspot) activity.

It was noted in Section III that the Helios 1 second solar conjunction noise data were biased upward from the $NOISE_p$ model, and that a model equal to

$$1.5 \times NOISE_p$$

gave a more reasonable fit to the data. This can be explained by the overall increase in solar activity between the early 1975 data to which $NOISE_p$ was originally fit and the August–October 1975 period of the second Helios 1 solar conjunction. During the earlier period, the flux and sunspot activity averaged

$$\text{Ottawa flux} = 71.1$$
$$R_Z = 8.3$$

while during the latter period, the average indice values were

$$\text{Ottawa flux} = 85.0$$
$$R_Z = 26.7$$

This increased activity affords the opportunity to make some very gross conjectures for the Mariner Jupiter/Saturn (MJS) period and the Pioneer 11 Saturn Encounter.

Figure 7 shows the past 12 years of solar activity in terms of R_Z, and B. Madsen in Ref. 3 indicates that the prediction for the next solar cycle calls for a maximum smoothed sunspot number of approximately 100. Considering that during July and August 1975 the sunspot activity quickened to an average of about

$$R_Z \sim 34$$

with a maximum of

$$R_Z = 104$$

and based on the Helios 1 observed doppler noise during this period, one might tentatively consider the following to be very approximate upper bounds to the expected doppler noise during the active portion of the next sunspot cycle:

R_Z average	Expected noise
50	$\lesssim 2.0 \times NOISE_p$
100	$\lesssim 4.0 \times NOISE_p$

V. Summary

This report analyzes the solar effects on the doppler data during the second Helios 1 solar conjunction. The doppler noise is shown to fit the previously presented $NOISE_p$ model, although at an elevated level

$$\text{Observed doppler noise} \propto 1.5 \times NOISE_p$$

This results from the fact that the average solar activity during July and August 1975 was considerably higher than the level in effect during the early 1975 solar conjunctions—the earlier data being those to which the $NOISE_p$ model was originally scaled. From this change in average level of solar activity, one can make some extremely tentative guesses as to the magnitude of solar corruption of doppler data during the next solar cycle, these being

R_Z average	Expected noise
50	$\lesssim 2.0 \times NOISE_p$
100	$\lesssim 4.0 \times NOISE_p$

Finally, strong similarities are seen between observed solar activity (in this case, R_Z) and deviations from the $NOISE_p$ model.

References

1. Berman, A. L., and Rockwell, S. T., "Analysis and Prediction of Doppler Noise During Solar Conjunctions," in *The Deep Space Network Progress Report 42-30*, pp. 231–263, Jet Propulsion Laboratory, Pasadena, Calif., Dec. 15, 1975.
2. Berman, A. L., and Rockwell, S. T., "Correlation of Doppler Noise During Solar Conjunctions With Fluctuations in Solar Activity," in *The Deep Space Network Progress Report 42-30*, pp. 264–272, Jet Propulsion Laboratory, Pasadena, Calif., Dec. 15, 1975.
3. Madsen, B., "Predicted Effect of the Solar Corona on MJS Telecommunications Performance," IOM 3396-75-171, Jet Propulsion Laboratory, Pasadena, Calif., Oct. 14, 1975 (an internal document).

Bibliography

Winn, F. B., et al., "Corruption of Radio Metric Doppler Due to Solar Plasma Dynamics: S/X Dual Frequency Doppler Calibration For These Effects," in *The Deep Space Network Progress Report 42-30*, pp. 88–101, Jet Propulsion Laboratory, Pasadena, Calif., Dec. 15, 1975.

Acknowledgments

The author would like to acknowledge S. T. Rockwell, who processed the data, and M. F. Cates, who executed the illustrations.

Table 1. Heilos 1 second solar conjunction 1975

Deep Space Station (DSS)	Day of year (DOY)	Average doppler noise, Hz	Sun–Earth–probe angle, deg	Earth–Sun–probe angle, deg	Integrated solar intensity (ISI)
11	215	0.0573	7.130	163.911	1321
11	216	0.0462	7.052	163.998	1336
11	219	0.0323	6.757	164.393	1397
11	220	0.0350	6.638	164.571	1424
11	223	0.0525	6.198	165.286	1531
11	224	0.0792	6.030	165.581	1576
11	225	0.0455	5.839	165.923	1631
11	226	0.0304	5.647	166.280	1690
11	235	0.1964	3.147	171.642	3127
11	274	0.0033	20.612	47.014	133
11	276	0.0037	20.743	40.222	114
12	228	0.0603	5.234	167.077	1832
14	210	0.0290	7.375	163.751	1276
14	212	0.0282	7.301	163.766	1289
14	213	0.0295	7.250	163.799	1298
14	214	0.0220	7.191	163.849	1309
14	217	0.0718	6.962	164.111	1354
14	221	0.0455	6.501	164.784	1455
14	222	0.0342	6.345	165.038	1493
14	227	0.0537	5.432	166.691	1761
14	231	0.0725	4.434	168.730	2182
14	234	0.7752	3.548	170.702	2758
14	239	1.4350	1.502	175.783	6706
14	241	5.0200	0.590	178.300	17,315
14	244	0.9230	0.989	177.006	10,255
14	246	0.3180	2.171	173.183	4572
14	247	0.1915	2.831	170.928	3461
14	248	0.0870	3.435	168.783	2817
14	250	0.0423	4.895	163.270	1913
14	251	0.0328	5.482	160.906	1684
14	252	0.0255	6.327	157.375	1428
14	254	0.0240	7.954	150.045	1084
14	255	0.0178	8.705	146.403	967
14	256	0.0168	9.542	142.154	857
14	257	0.0107	10.410	137.512	761
14	258	0.0137	11.433	131.734	665
14	259	0.0225	12.166	127.330	604
14	260	0.0140	13.003	122.057	542
14	261	0.0127	13.846	116.454	487
14	262	0.0163	14.806	109.687	429
14	264	0.0088	16.306	98.075	349
14	265	0.0072	17.006	92.148	315
14	266	0.0055	17.746	85.444	280
14	267	0.0063	18.263	80.384	256
14	269	0.0043	19.270	69.349	210

Table 1 (contd)

Deep Space Station (DSS)	Day of year (DOY)	Average doppler noise, Hz	Sun–Earth–probe angle, deg	Earth–Sun–probe angle, deg	Integrated solar intensity (ISI)
14	270	0.0037	19.713	63.680	189
14	271	0.0033	20.001	59.464	174
14	273	0.0022	20.470	50.831	145
14	275	0.0028	20.698	43.629	123
14	277	0.0020	20.735	36.728	104
42	210	0.0353	7.368	163.749	1277
42	212	0.0242	7.288	163.773	1291
42	214	0.0683	7.178	163.862	1311
42	216	0.0295	7.021	164.035	1342
42	227	0.0413	5.377	166.798	1780
42	228	0.0387	5.152	167.240	1862
42	233	0.1988	4.061	169.542	2394
42	234	0.2502	3.401	171.044	2883
42	237	0.5162	2.310	173.695	4309
42	249	0.2225	3.663	167.945	2629
43	224	0.0507	6.158	165.356	1541
43	225	0.0493	5.982	165.666	1590
43	225	0.0390	5.783	166.027	1648
43	249	0.2470	3.591	168.209	2686
43	250	4.7112	4.224	165.860	2252
43	255	0.0178	8.215	148.782	1041
43	256	0.0142	8.128	149.207	1055
43	257	0.0133	9.812	140.739	826
43	258	0.0143	10.701	135.897	753
43	260	0.0158	12.403	125.871	586
43	261	0.0182	13.310	120.060	522
43	262	0.0180	14.164	114.266	467
43	263	0.0137	14.992	108.310	419
43	264	0.0098	15.833	101.878	373
43	265	0.0085	16.520	96.305	339
43	266	0.0063	17.300	89.529	301
43	267	0.0052	17.909	83.871	273
43	268	0.0042	18.481	78.146	247
43	269	0.0045	18.940	73.205	226
43	270	0.0046	19.401	67.739	204
43	271	0.0042	19.782	62.690	185
43	272	0.0043	20.100	57.867	168
43	273	0.0048	20.353	53.294	153
43	274	0.0035	20.514	49.770	142
43	275	0.0033	20.641	46.032	130
43	276	0.0028	20.716	42.643	121
43	277	0.0028	20.747	39.323	111
44	229	0.0468	4.902	167.945	1963

Table 1 (contd)

Deep Space Station (DSS)	Day of year (DOY)	Average doppler noise, Hz	Sun–Earth–probe angle, deg	Earth–Sun–probe angle, deg	Integrated solar intensity (ISI)
61	210	0.0282	7.386	163.756	1274
61	213	0.0230	7.269	163.786	1294
61	215	0.0450	7.151	163.889	1317
61	216	0.0763	7.079	163.967	1330
61	218	0.1342	6.903	164.188	1366
61	219	0.0478	6.785	164.353	1391
61	220	0.0363	6.666	164.529	1417
61	221	0.0655	6.551	164.705	1444
61	222	0.0320	6.412	164.929	1477
61	223	0.0495	6.251	165.197	1517
61	225	0.0420	5.928	165.763	1605
61	226	0.0387	5.709	166.165	1670
61	227	0.0475	5.520	166.521	1731
61	228	0.0482	5.291	166.966	1811
61	229	0.0435	5.056	167.435	1900
61	232	0.0783	4.265	169.096	2274
61	234	0.3895	3.672	170.419	2661
61	250	0.0443	4.626	164.312	2037
61	272	0.0037	20.206	56.041	162
61	274	0.0025	20.578	47.959	136
61	275	0.0025	20.684	44.211	125
61	276	0.0027	20.735	40.895	115
61	277	0.0022	20.747	38.207	108
63	254	0.0380	7.681	151.306	1132
63	258	0.0173	10.994	134.232	704
63	262	0.0177	14.511	111.791	446
63	266	0.0052	17.503	87.672	292
63	269	0.0038	19.138	70.891	216
63	270	0.0037	19.585	65.346	195

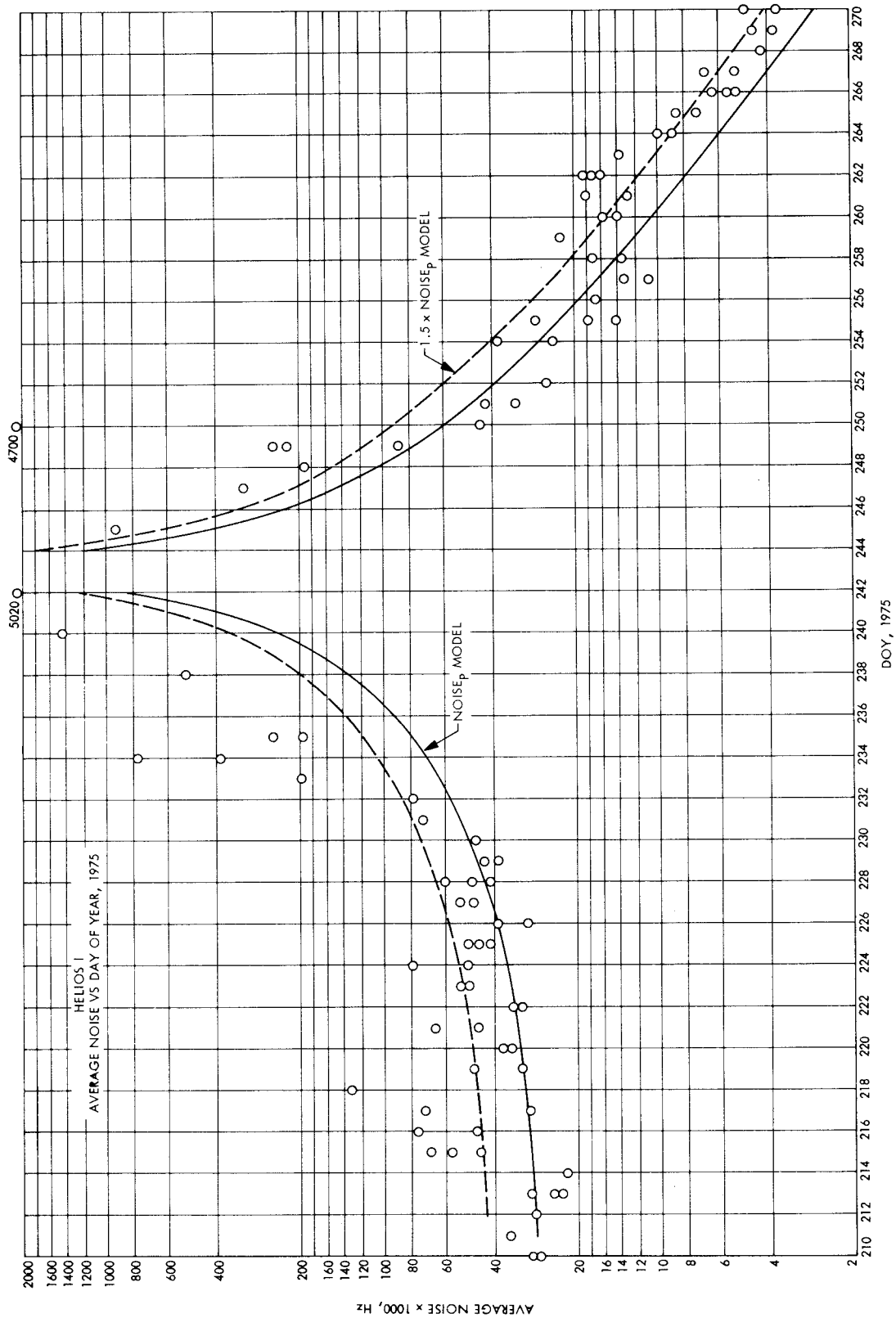

Fig. 1. Average noise vs day of year, 1975

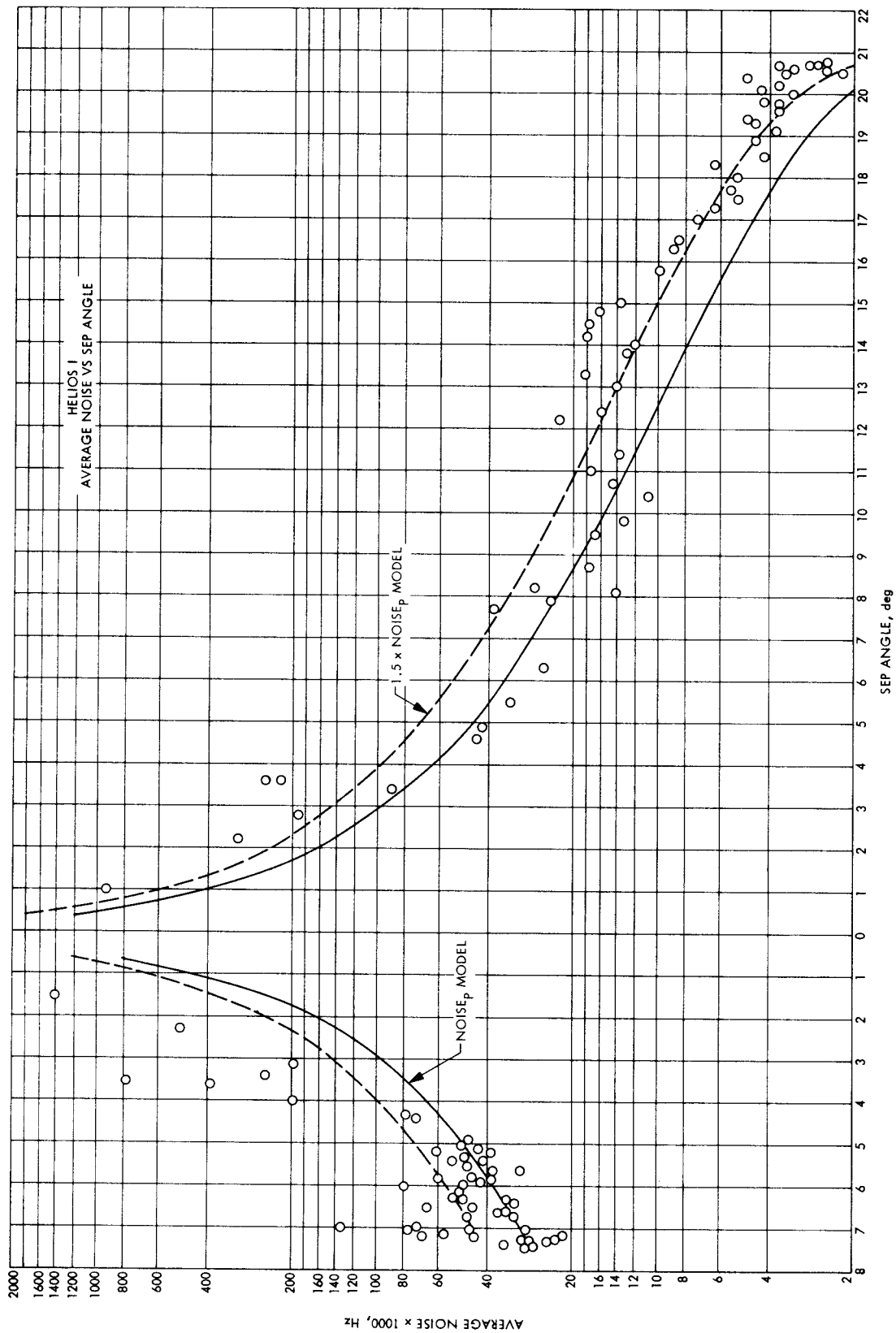

Fig. 2. Average noise vs SEP angle

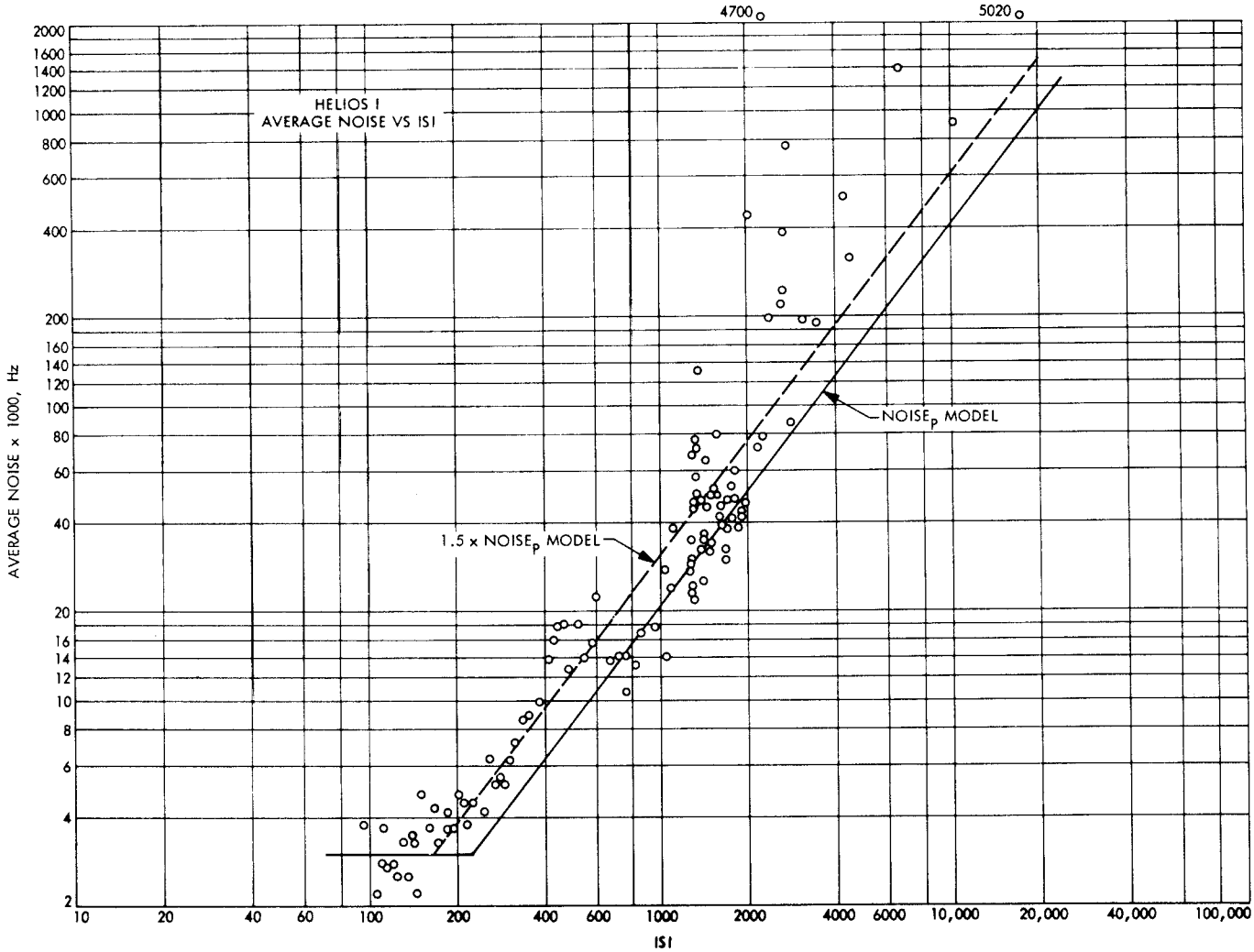

Fig. 3. Average noise vs ISI

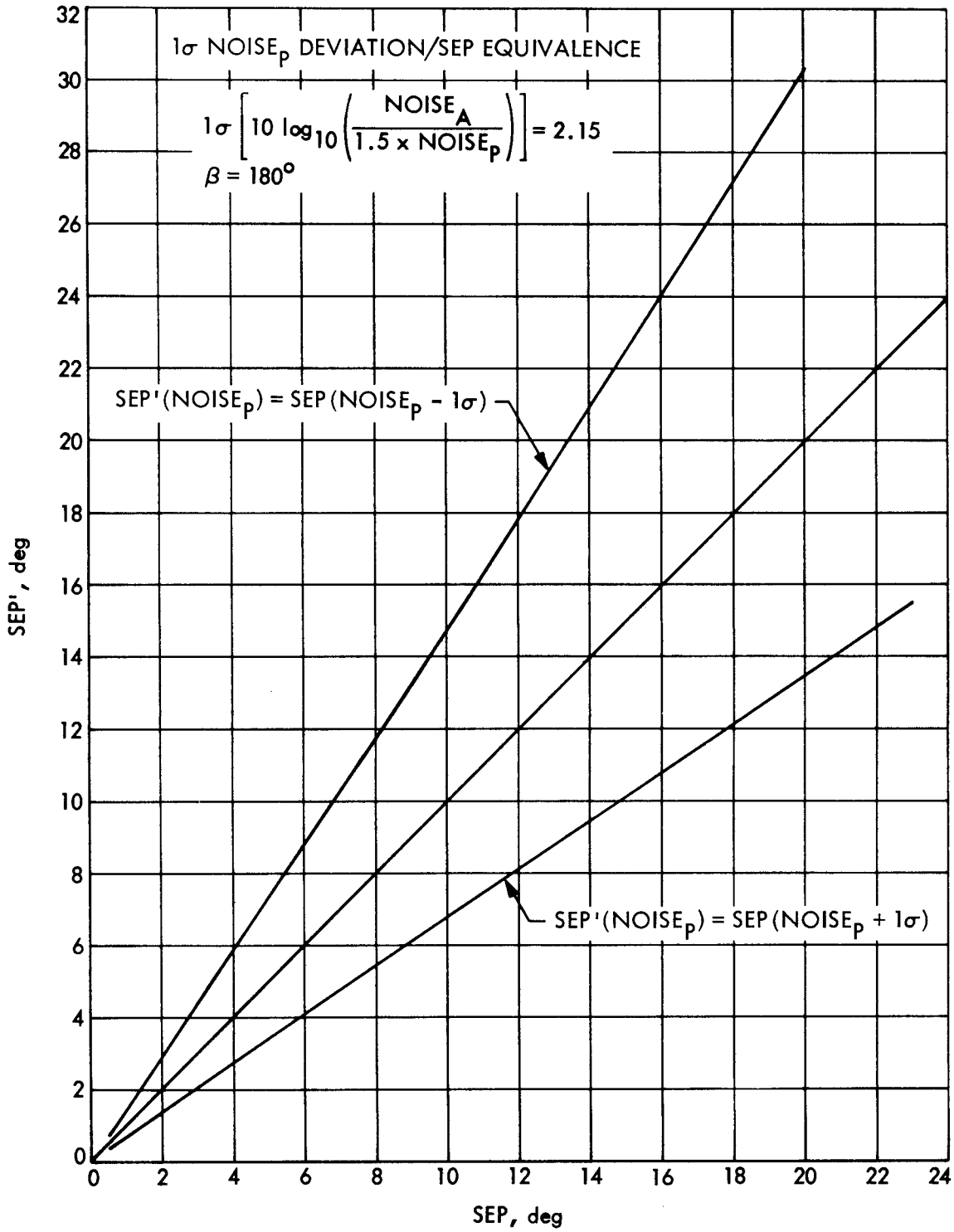

Fig. 4. Equivalent SEP angles for 1σ *NOISE$_p$* deviations

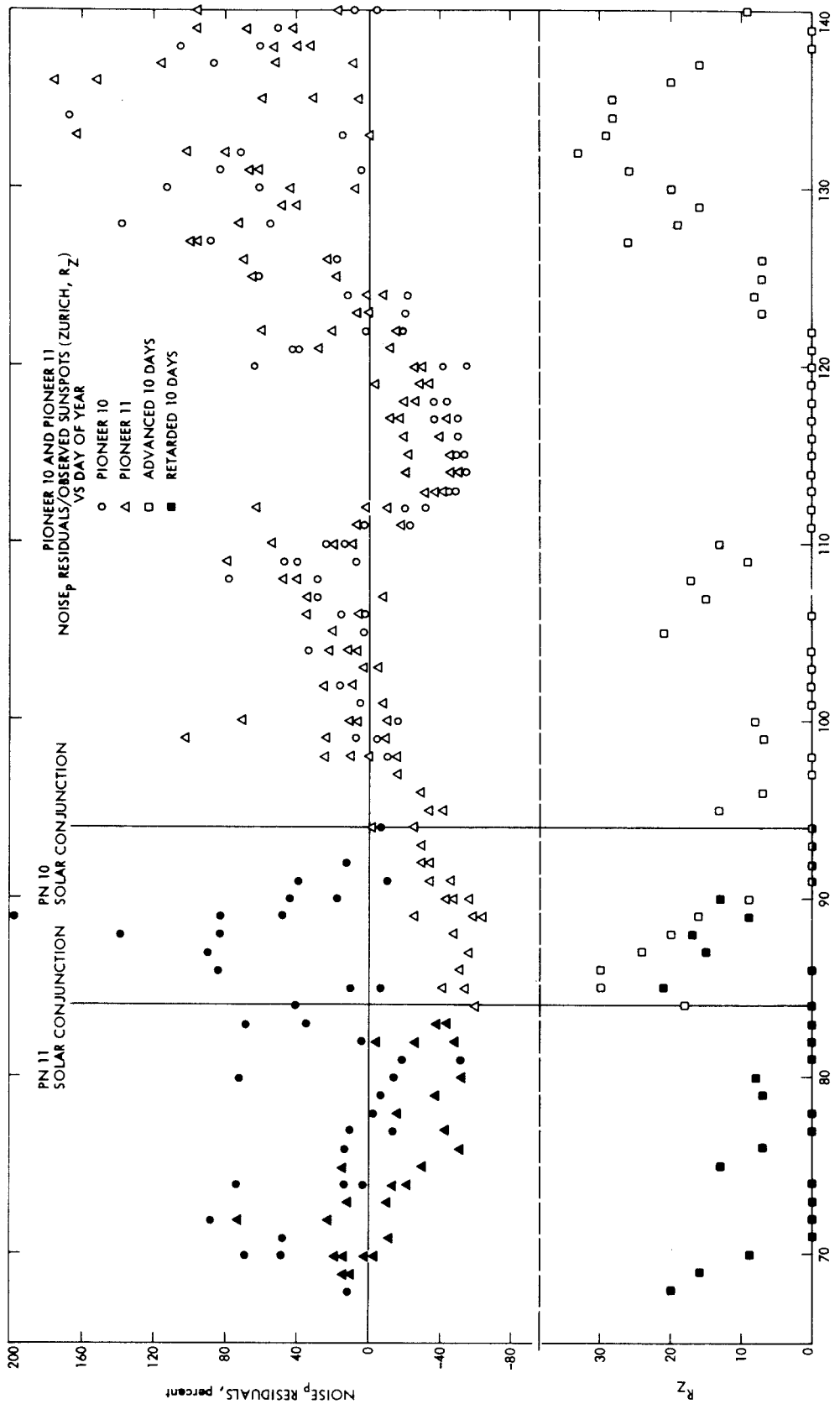

Fig. 5. Pioneer 10/11 *NOISE*$_p$ residuals and observed sunspots vs day of year

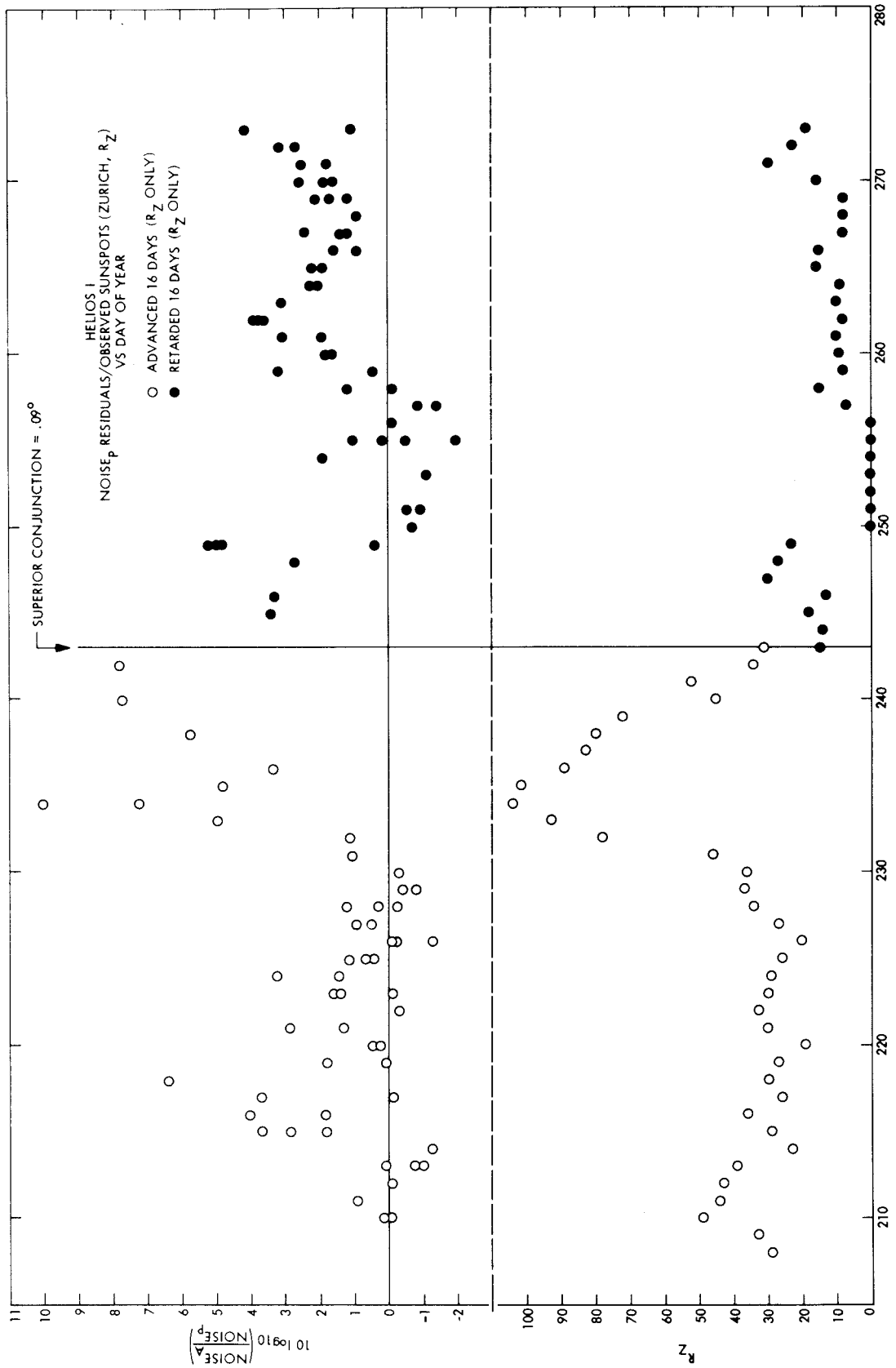

Fig. 6. Helios 1 *NOISE*$_P$ residuals and observed sunspots vs day of year

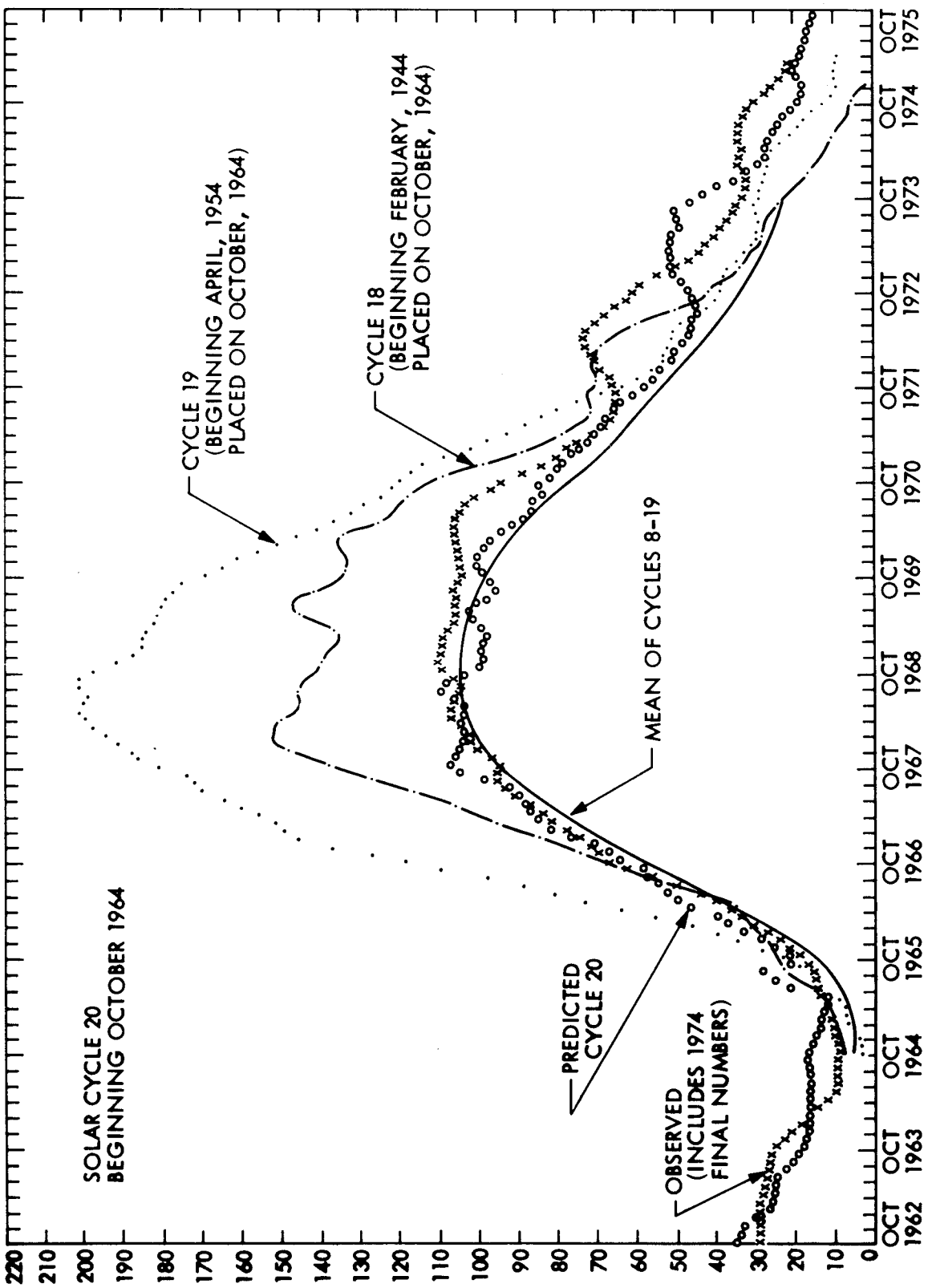

Fig. 7. Predicted and observed sunspot activity, 1962–1975